

A Unique Presentation of Multiple Endocrine Neoplasia Type 2A

AUTHORS:Martin G^a; Rafii D^b; Romero Arenas MA^{a,c}**CORRESPONDING AUTHOR:**

Minerva A. Romero Arenas, MD, MPH, FACS
 Department of Surgery
 Weill Cornell Medicine
 1300 York Avenue
 New York, NY 10065
 Email: mar9462@med.cornell.edu

AUTHOR AFFILIATIONS:

a. Department of Endocrine Surgery
 NewYork-Presbyterian Brooklyn Methodist Hospital
 Brooklyn, NY 11215

b. Department of Medicine
 Division of Endocrinology
 NewYork-Presbyterian Brooklyn Methodist Hospital
 Brooklyn, NY 11215

c. Weill Cornell Medicine
 New York, NY 10065

Background	<p>Multiple endocrine neoplasia type 2 (MEN2) is an autosomal dominant disorder due to a genetic defect in the RET proto-oncogene, causing multicentric tumor formation in organs where the RET gene is expressed. There are two main types of MEN2, which are distinguished by their clinical presentation:</p> <ul style="list-style-type: none"> • MEN2A: This form accounts for approximately 95% of MEN2 cases. It is characterized by a triad of tumors: medullary thyroid cancer (MTC) arising from the thyroid gland, pheochromocytoma (PCC) developing in the adrenal glands, and primary hyperparathyroidism (PHPT) involving the parathyroid glands. MTC is typically the first manifestation of the disease. MEN2A-associated PCCs are usually benign, meaning they are unlikely to spread to other parts of the body. Additionally, PHPT in MEN2A is often mild, affecting one to four parathyroid glands. • MEN2B (MEN2B): This less frequent form of MEN2 presents with a different constellation of findings. In addition to MTC and PCC, patients with MEN2B also develop mucosal neuromas and marfanoid habitus. This subtype is notable for the absence of PHPT. <p>The estimated prevalence of MEN2A is about 1/40,0000, while MEN2B varies between 1/350,000 to 1/700,000.</p>
Summary	<p>This case report describes a unique presentation of MEN2A in a 47-year-old woman. She initially presented to the emergency department with a hypertensive emergency and bilateral adrenal hemorrhage. Upon admission, doctors diagnosed her with three synchronous tumors: bilateral pheochromocytomas, medullary thyroid carcinoma, and a parathyroid adenoma. After stabilization and discharge, she underwent bilateral adrenalectomy followed by total thyroidectomy with parathyroidectomy. Genetic testing confirmed a mutation at codon 634 of the RET proto-oncogene, the most common mutation for MEN2A. Interestingly, the patient also displayed megacolon and features of a marfanoid habitus.</p>
Conclusion	<p>This case highlights the heterogeneity MEN2A can present. Our patient displayed all three endocrine neoplasms (PCC, MTC, PHPT) simultaneously, nearly a decade later than the mean diagnostic age for each individual tumor, likely attributed to challenges in accessing specialized care. Additionally, she had features typically seen in MEN2B, such as marfanoid habitus and megacolon. While megacolon is rare in MEN2A and usually associated with mutations on exon 10, this report describes the first documented case of megacolon associated with the most common MEN2A mutation (codon 634 on exon 11).</p>
Key Words	hereditary syndromes; pheochromocytoma; medullary thyroid carcinoma; hyperparathyroidism; marfanoid habitus; megacolon
Abbreviations	CKMB: creatine kinase-myocardial band, TSH: thyroid-stimulating hormone, T4: tetraiodothyronine, TI-RADS: Thyroid Imaging, Reporting and Data System, ATA: American Thyroid Association

DISCLOSURE STATEMENT:

The authors have no conflicts of interest to disclose.

FUNDING/SUPPORT:

The authors have no relevant financial relationships or in-kind support to disclose.

RECEIVED: November 3, 2022

REVISION RECEIVED: June 5, 2023

ACCEPTED FOR PUBLICATION: June 27, 2023

To Cite: Martin G, Rafii D, Romero Arenas MA. A Unique Presentation of Multiple Endocrine Neoplasia Type 2A. *ACS Case Reviews in Surgery*. 2024;4(8):105-112.

Case Description

A 47-year-old African American woman with a past medical history of long-standing hypertension, type 2 diabetes, hyperlipidemia, chronic mild hypercalcemia, and a multinodular goiter (biopsied 10 years prior, showing benign tissue) presented to the emergency department (ED) with a constellation of concerning symptoms. Over the past three weeks, she had experienced progressive malaise, generalized weakness, and lightheadedness, with two syncopal falls at home in the preceding week. Additionally, she reported headaches, nausea, vomiting, abdominal pain, anorexia, weight loss, and severe constipation (not having a bowel movement for 3-4 weeks).

Upon arrival in the ED, her vital signs revealed high blood pressure (203/140 mm Hg), tachycardia (110 beats per minute), and tachypnea (22 breaths per minute). A physical examination showed a tall, slender build and mild distress. Notably, she had an enlarged, irregularly shaped thyroid gland with soft, palpable nodules bilaterally and a diffusely tender abdomen upon palpation.

Laboratory values were notable for hyperglycemia (308 mg/dL), signs of acute kidney injury (elevated creatinine, 1.64 mg/dL), hyponatremia (126 mEq/L), hypochloremia (89 mEq/L), hypercalcemia (corrected 11.3 mEq/L), elevated cardiac enzymes (CKMB 15.2 IU/L, troponin 0.19 ng/mL), and hyperlactatemia (4.3 mg/dL). Her thyroid function tests, TSH (0.747 mIU/mL) and free T4 (0.83 ng/dL), were within the normal range.

An abdominal and pelvic CT scan was performed, which demonstrated enlarged bilateral adrenal glands (right: 7.0 × 6.9 × 10.8 cm, left: 9.4 × 9.5 × 8.7 cm) with internal heterogeneous hypodensities, concerning for bilateral adrenal hemorrhage, and a markedly dilated rectum measuring up to 10.1 cm in transverse diameter (Figure 1).

Further endocrine work-up revealed elevated levels of plasma metanephrines (total >40,000 pg/mL, normetanephrine >15,000 pg/mL), calcitonin (>4500 pg/mL), carcinoembryonic antigen (CEA, 26 ng/mL), and parathyroid hormone (PTH, 311 pg/mL). Additional labs showed normal aldosterone (1.3 ng/mL), elevated renin (28.12 ng/mL/hr), with a low aldosterone-to-renin ratio (0.05), normal cortisol (AM 98 mcg/dL), normal phosphorus (3.2 mEq/L), and normal vitamin D levels (35.5 ng/mL).

Figure 1. Abdominopelvic CT Reveals Marked Rectal Distention with Fecal Impaction (red arrow). Published with Permission



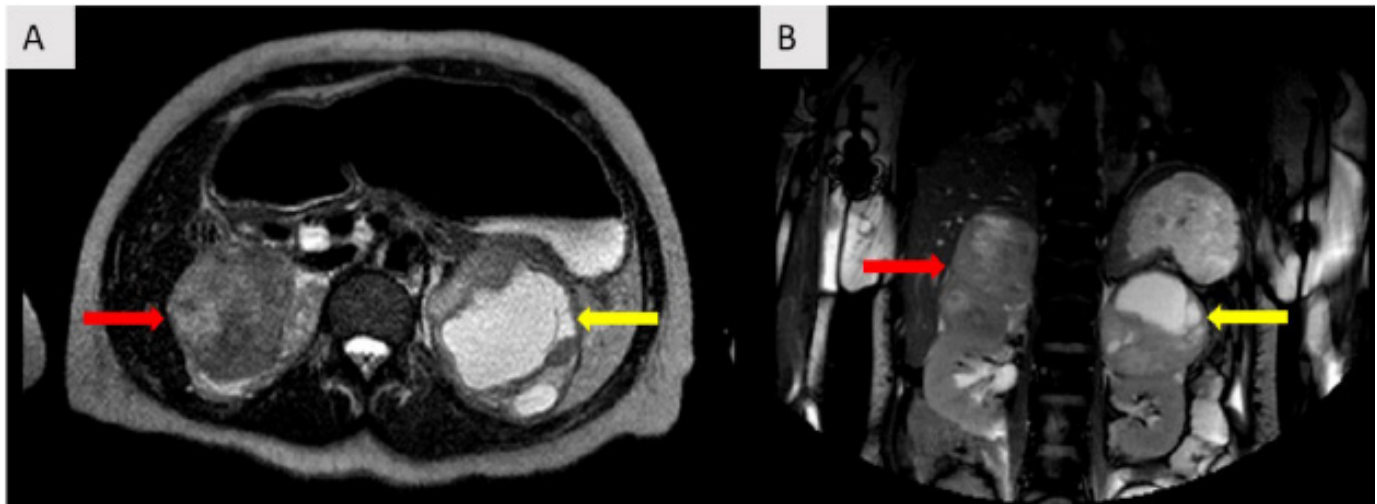
The rectum measures approximately 10.1 cm in diameter.

The patient was admitted to the medical ICU for hypertensive emergency and stabilized on nicardipine infusion, which was transitioned days later to a combination of oral nifedipine, doxazosin, and labetalol. An MRI scan of the abdomen and pelvis further defined the adrenal findings as bilateral lobulated, exophytic T2-intense lesions arising from the adrenal glands with cystic areas, consistent with hemorrhagic product (Figure 2).

Compared to outside imaging from twelve years prior, an ultrasound examination of the thyroid gland during this admission identified an interval upgrade in TI-RADS classification of a right thyroid nodule from TI-RADS 4 to TI-RADS 5 (presence of internal micro and macro-calcifications, suggestive of malignancy). Additionally, a left thyroid nodule showed slight enlargement but remained classified as TI-RADS 4 (Figure 3).

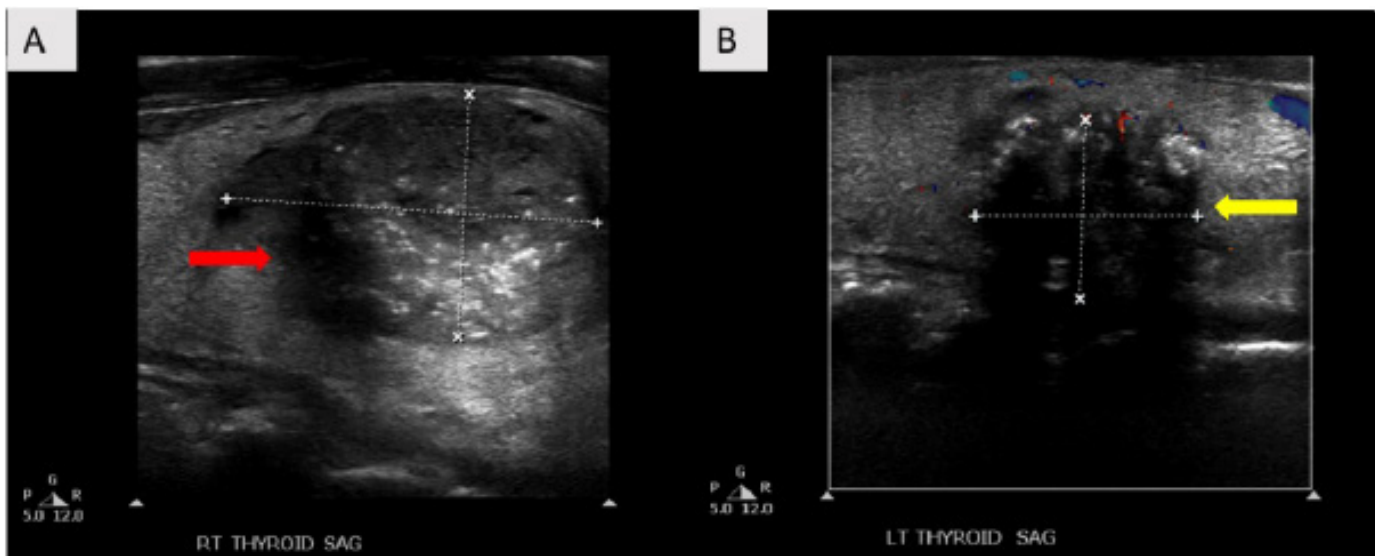
The combination of pheochromocytoma (indicated by the bilateral adrenal masses and significantly elevated plasma metanephrine levels), primary hyperparathyroidism (elevated PTH and hypercalcemia), and medullary thyroid cancer (highly suspicious thyroid nodules with hypercalcitoninemia) led to a clinical diagnosis of MEN2A. Genetic testing samples were collected before the patient's discharge, and subsequent analysis confirmed a mutation in the RET proto-oncogene at codon 634 (C634W, ATA Risk Level C¹³).

Figure 2. Adrenal Gland Masses Demonstrated on MRI. Published with Permission



A) Axial and B) coronal MRI showing a 7.4 × 7.2 × 11.6 cm heterogeneous mildly T2 hyperintense lobulated lesion arising from the right adrenal gland (red arrows). A 9.9 × 9.1 × 8.3 cm heterogeneous lobulated exophytic lesion with an area of cystic/necrotic changes arising from the left adrenal gland (yellow arrows). These lesions likely contain hemorrhagic complement.

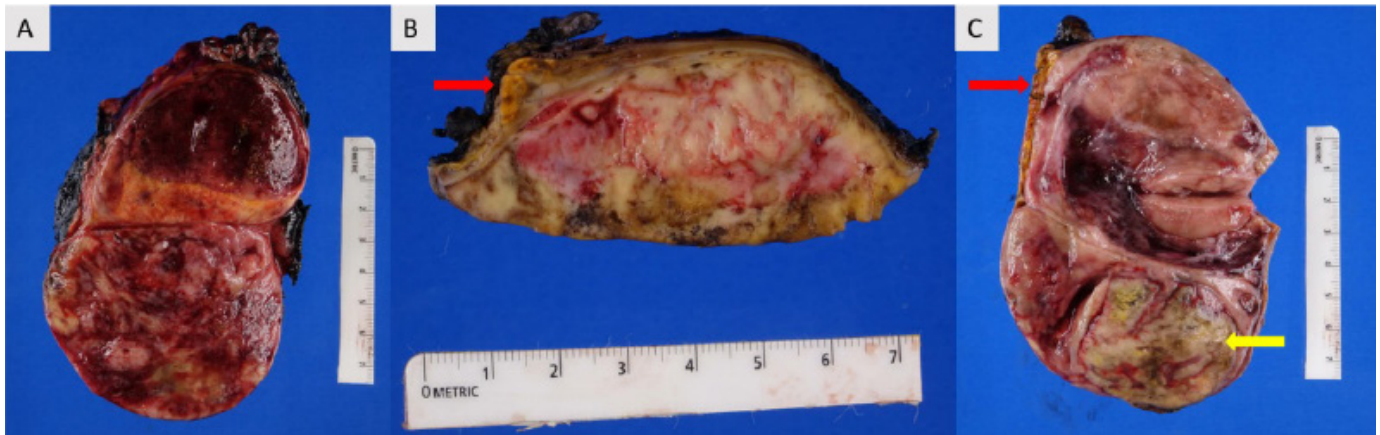
Figure 3. Thyroid Nodules on Ultrasound. Published with Permission



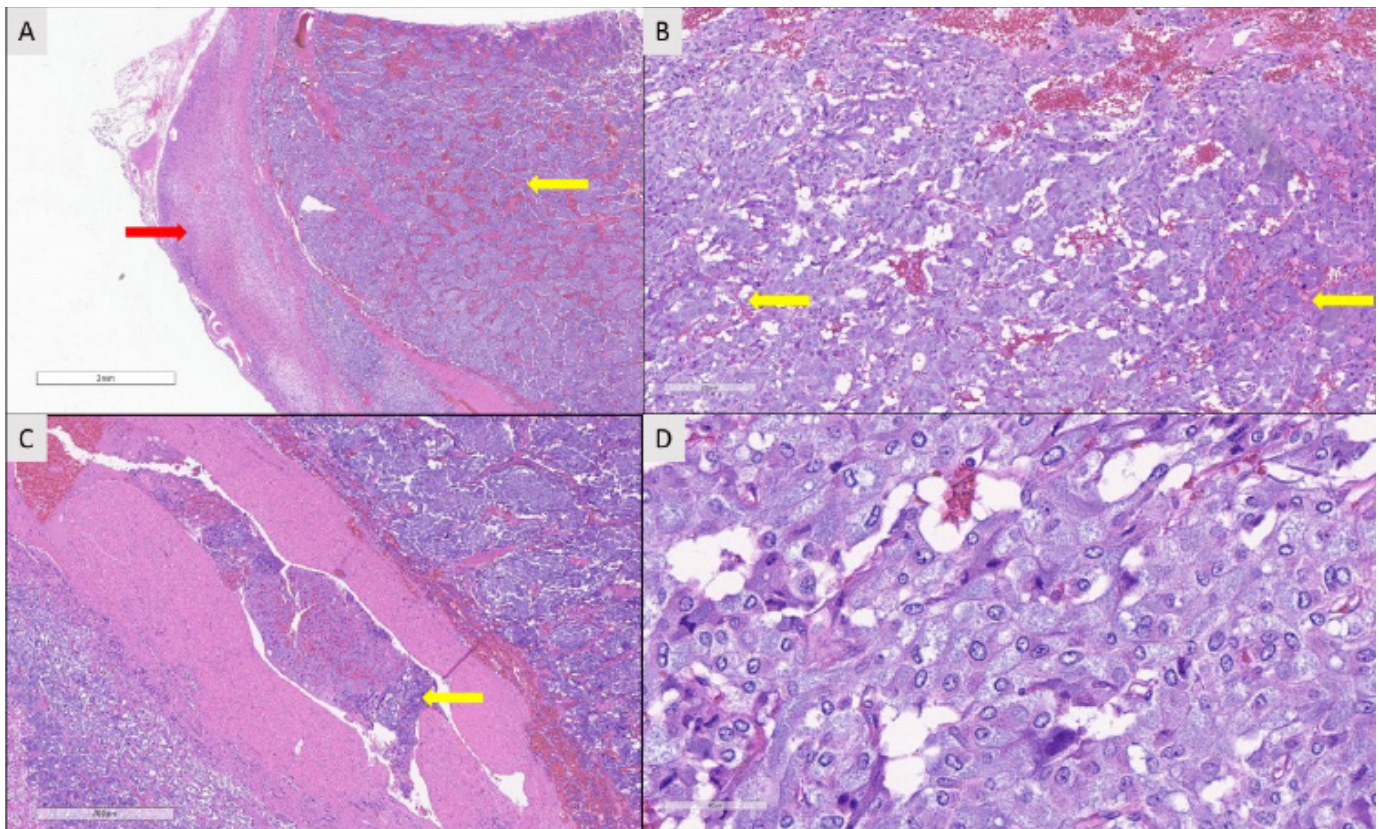
A) Right thyroid lobe containing a 4.2 × 2.5 × 2.6 cm solid, heterogeneous nodule (red arrow). The solid components are hypoechoic to the parenchyma. Large echogenic foci within the nodule cast acoustic shadows, consistent with macrocalcifications. Additionally, smaller punctate echogenic foci suggestive of microcalcifications are present (TI-RADS 5). B) Left thyroid lobe containing a 2.7 × 1.6 × 2.0 cm solid, hypoechoic, and heterogeneous nodule (yellow arrow). Macrocalcifications are visualized within the nodule (TI-RADS 4).

Following medical optimization, the patient underwent laparoscopic bilateral adrenalectomy. Pathological examination of the removed tissue confirmed the presence of pheochromocytomas (PCC) in both adrenal glands.

The tumors measured 12.2 cm and 10.4 cm on the right and left sides, respectively, and originated from the adrenal medulla (Figures 4 and 5).

Figure 4. Gross Findings of Bilateral Pheochromocytomas. Published with Permission

A) Right adrenal gland demonstrating a bilobed pheochromocytoma with a heterogeneous red-tan and focally hemorrhagic cut surface. B) Sagittal view of the right adrenal gland. The pheochromocytoma occupies the majority of the gland, with only a small rim of normal-appearing golden-yellow adrenal cortex visible at the upper left border (red arrow). C) Left adrenal gland with a pheochromocytoma exhibiting a more cystic appearance compared to the right. The pheochromocytoma demonstrates pronounced green-tinged necrosis at the inferior aspect (yellow arrow) and again, the golden-yellow adrenal cortex is visible at the upper left margin.

Figure 5. Histopathological Findings of Right Adrenal Pheochromocytoma. Published with Permission

A) Low-power image showing the right adrenal gland. The normal adrenal cortex is visible on the left (red arrow), and the pheochromocytoma (tumor) is visible on the right (yellow arrow). B) Moderate-power image highlighting the characteristic "zellballen nests" (yellow arrows) of the pheochromocytoma. These are clusters of tumor cells surrounded by a delicate fibrovascular stroma. C) Moderate-power image showing tumor cells within a blood vessel (yellow arrow), indicating lymphovascular invasion. This finding was specific to the right adrenal gland. D) High-power image of tumor cells exhibiting a relatively low nuclear-to-cytoplasmic ratio, with round nuclei containing occasional pseudoinclusions. The cytoplasm appears granular and ranges from amphophilic to basophilic staining. No significant increase in mitoses is observed.

Following successful bilateral adrenalectomy, the patient was started on adrenal replacement therapy (oral prednisone and fludrocortisone). Further evaluation focused on the diagnosis and management of medullary thyroid carcinoma (MTC).

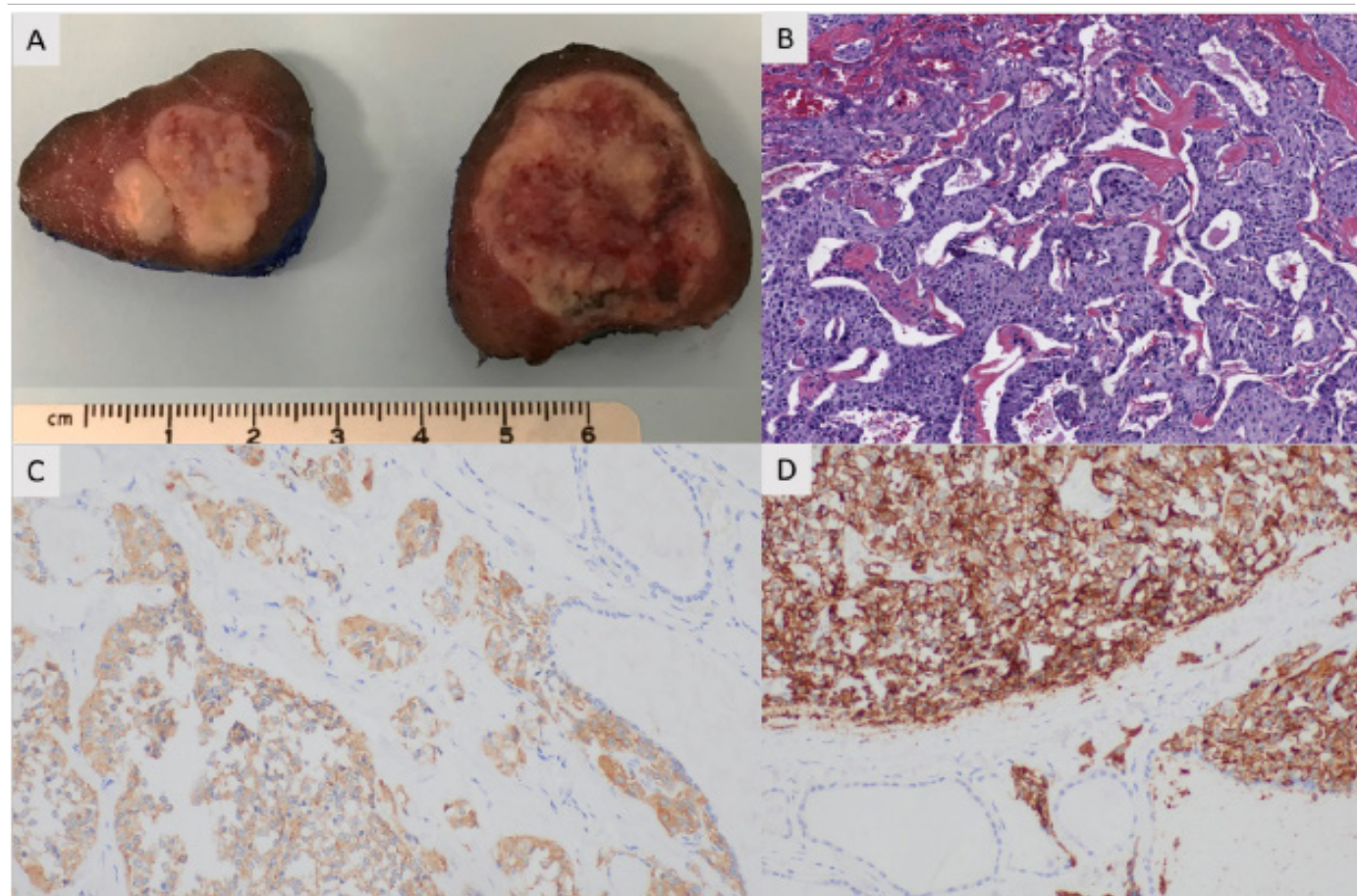
Outpatient investigations included ultrasound-guided fine needle aspirations (FNA) of suspicious thyroid nodules, which were classified as benign follicular nodules (Bethesda II/VI). Sestamibi imaging did not reveal any evidence of parathyroid adenoma. CT scan of the neck identified two possible parathyroid glands along the left paraesophageal groove. There was no radiologic evidence of abnormal lymph nodes.

Based on these findings, the decision was made to proceed with surgery. The surgical approach included a standard cervical exploration for parathyroidectomy and total thyroidectomy with bilateral central neck lymphadenectomy.

During surgery, four parathyroid glands were visualized and examined. Three appeared normal in size, morphology, and color. However, one enlarged parathyroid gland (located in the left inferior position) was identified and removed. This removal led to a confirmatory drop in intraoperative PTH levels from 152 pg/mL to 10 pg/mL. No supernumerary glands were found upon careful search along the resection bed.

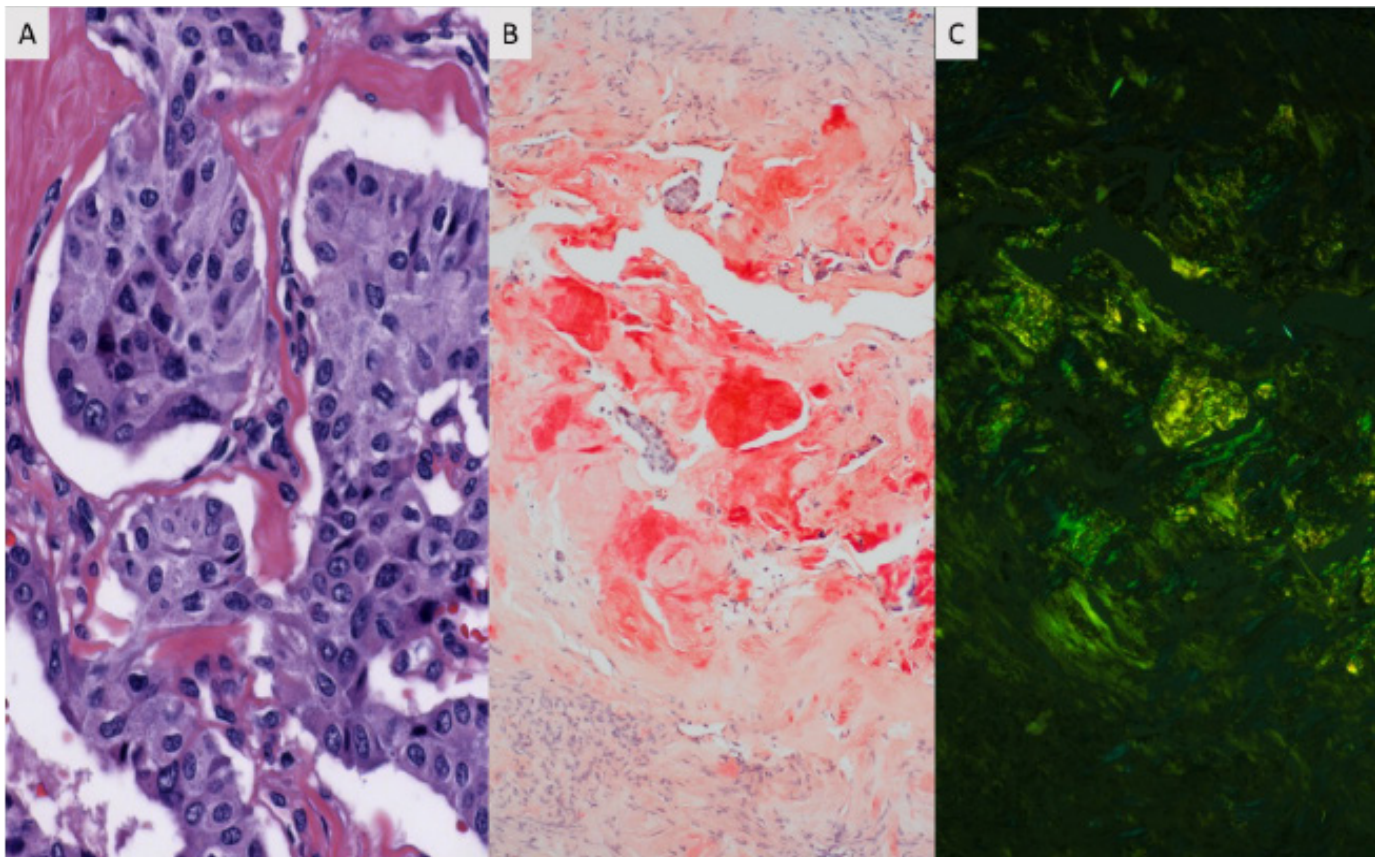
Pathological examination of the surgical specimens revealed a hypercellular parathyroid gland consistent with a parathyroid adenoma. Additionally, medullary thyroid carcinoma was identified arising from both the right (4.7 cm) and left (2.7 cm) thyroid lobes (Figures 6 and 7). Furthermore, three lymph nodes showed positive results for metastatic MTC, with involvement of tissues beyond the lymph node capsule (pT2 pN1a cM0). No additional parathyroid tissue was found within the central neck specimen.

Figure 6. Pathological Findings of MTC. Published with Permission



A) Gross photograph of the resected thyroid gland. The specimen shows a solid, hemorrhagic tumor mass involving both the left and right thyroid lobes. **B)** Microscopic examination (H&E stain, 200x magnification) reveals sheets and cords of tumor cells with eosinophilic amorphous material, a characteristic feature of MTC. **C & D)** Immunostains for neuroendocrine markers (synaptophysin and chromogranin, respectively) confirming the diagnosis of MTC.

Figure 7. Histopathological findings consistent with MTC. Published with Permission



A, 400x magnification) Congo red stain demonstrates amyloid deposition (red) within the MTC tissue. B) Congo red stain reveals characteristic apple-red birefringence of amyloid deposits. C) Polarized light microscopy confirms the presence of amyloid with apple-green birefringence.

Postoperatively, the patient was monitored closely with physical exam, biochemical testing, and neck ultrasound every six months. Normocalcemia was confirmed at six months following parathyroidectomy without evidence of recurrence (calcium 8.7 mg/dL). Tumor markers dropped precipitously (most recent calcitonin 8.7 pg/mL and CEA 3.7 ng/mL).

Genetic counseling and cascade testing were offered to the patient's family. The patient's daughter was found to carry the same mutation at codon 634. Her disease manifested as PHPT and MTC, without evidence of pheochromocytoma, and had already progressed to stage IV MTC with multiple bony metastases. Additional family members declined counseling and testing.

Discussion

In the human genome, the most frequently-identified RET mutation responsible for MEN2A involves the substitution of cysteine at codon 634 on exon 11.¹ While this mutation is well-established in MEN2A, this case report presents the first documented instance of megacolon associated with this specific mutation.

Megacolon is a known complication in MEN2B, affecting up to 63% of patients.² However, its occurrence in MEN2A is rare, and previously reported cases have linked the phenotype to mutations within exon 10 of the RET gene and more seldom at codons 609, 611, and 618. This case opens up the possibility that the most common MEN2A mutation (codon 634) might also be a potential culprit in the development of megacolon within the MEN2A spectrum, highlighting the phenotypic heterogeneity of the disease.³

Our patient exhibited several physical characteristics of marfanoid habitus, including tall stature (over six feet), elongated limbs, arachnodactyly, a highly arched palate, overcrowded teeth, and right-eye blindness from an early age. While rare, there have been other documented cases in which individuals with MEN2A exhibit marfanoid characteristics, suggesting some degree of clinical overlap between the two related syndromes. Giani and coauthors reported a similar case involving a de novo deletion in exon 11 of the RET gene. In addition to PHPT (as expected in MEN2A), this patient also displayed a marfanoid habitus, megacolon, and mucosal neuromas (typical of the MEN2B subtype).¹

Probands with MEN2A are usually diagnosed with MTC before the age of 35. Half of patients develop pheochromocytoma(s) by a mean age of 37, with 40% diagnosed concurrently with MTC. Primary hyperparathyroidism (PHPT) occurs in only about 25% of MEN2A patients, typically by age 38. This case report describes a unique presentation where the patient, a proband, was uniquely diagnosed with all three tumors (MTC, bilateral pheochromocytomas, and parathyroid adenoma) simultaneously at her initial hospitalization, at the much later age of 47. This significantly surpasses the expected age of diagnosis for any of the neoplasms that comprise MEN2A.^{4,5}

A concerning aspect of this patient's history is the presence of two negative thyroid biopsies performed over a decade before presenting to our team. While the false-negative rate for FNA biopsy in detecting papillary thyroid cancer is between 10% and 17%,⁶ the rate for medullary carcinoma can be as high as 43.6%.⁷ This significant discrepancy raises the question of whether additional testing, such as calcitonin measurements, might be beneficial in managing suspicious thyroid nodules. In this specific case, if the patient's calcitonin levels had been elevated and prompted a more comprehensive workup, her diagnosis could potentially have been established earlier. This earlier diagnosis might have significantly altered the prognosis for her daughter, potentially preventing the development of metastatic disease. This likely reflects disparities in access to specialized care and the need for high clinical suspicion for these rare clinical syndromes.

Bilateral Adrenalectomy: The large size of her bilateral pheochromocytomas (10.8 cm and 9.5 cm) traditionally might have warranted an open surgical approach for adrenalectomy. However, to minimize postoperative discomfort and shorten hospital stay,⁴ we opted for a laparoscopic approach.

This approach resulted in a successful surgery with minimal incisions, no wound complications, and discharge on postoperative day 4.

Lateral Neck Dissection: Given the patient's initial high calcitonin level (>4500 pg/mL) and the presence of nodules in both thyroid lobes, a dilemma arose regarding the necessity of a bilateral lateral neck dissection. This procedure can decrease the risk of needing future surgery for recurrent tumors.⁹ After careful discussion, the patient opted to defer this more extensive surgery. We felt close observation with regular biochemical monitoring and serial ultrasounds of the lateral neck (areas on either side of the thyroid) was reasonable, especially since preoperative imaging did not show concerning lymph nodes.

Parathyroid Surgery: Several factors informed our approach to the parathyroid disease. Preoperative discussions occurred in an interdisciplinary tumor board, and research supports selective removal of affected glands as an effective strategy in MEN2A patients compared to subtotal or total parathyroidectomy with autotransplantation. A study by O'Riordain et al. found no recurrence of PHPT in 18 MEN2A patients undergoing neck exploration at a median follow-up of 5.8 years, regardless of the surgical approach used (total vs. subtotal vs. selective resection).¹⁰ Similarly, another study by Raue et al. reported a recurrence rate of 12% at eight years, independent of the resection extent in MEN2A patients (n=67).¹¹ This contrasts with MEN1, where a higher risk of recurrence necessitates routine subtotal parathyroidectomy. In our patient's case, preoperative imaging was used, and all four parathyroid glands were closely evaluated during surgery. Real-time parathyroid hormone monitoring proved valuable. It helped guide the extent of dissection and confirm the suitability of selective excision with preservation of the remaining glands, thereby minimizing the risk of permanent hypothyroidism.¹²

Conclusion

This unique case of multiple endocrine neoplasia exemplifies the overlap between the two closely related syndromes, MEN2A and MEN2B. The patient's presentation displayed features of both subtypes, highlighting the phenotypic variability within MEN2. Additionally, this case expands the known spectrum of mutations potentially associated with the MEN2A-megacolon phenotype by identifying a mutation on exon 11, beyond the previously reported mutations on exon 10. This finding suggests a broader mutational landscape for this rare complication.

Furthermore, this case underscores the importance of recognizing the diverse presentations of MEN2A. This patient's indolent disease course, with a delayed diagnosis and synchronous presentation of all three endocrine tumors, deviates from the typical MEN2A picture. Practitioners should maintain a high index of suspicion for MEN2A.

Lessons Learned

This case highlights several crucial lessons for managing MEN2A. The patient's delayed diagnosis, occurring over a decade after initial thyroid biopsies, underscores the limitations of FNA in detecting MTC and a lack of access to specialized care. Adjunctive techniques may be necessary for reliable early diagnosis. Early genetic testing is essential for all close relatives of a diagnosed MEN2A patient to facilitate prompt treatment initiation.

Our surgical approach of this proband reinforces the benefits of prioritizing minimally invasive adrenalectomy whenever feasible. Additionally, selective parathyroidectomy with intraoperative PTH monitoring offers a reasonable approach to managing MEN2A-associated hyperparathyroidism. This approach has been shown to achieve low recurrence rates while minimizing the risk of permanent hypothyroidism.

Postoperative management should involve close surveillance with serial neck sonography and frequent biochemical monitoring. This case also emphasizes the importance of early detection and genetic counseling for at-risk family members, particularly due to the potential for advanced disease presentation in offspring.

Acknowledgments

We are grateful to Peilin Zhang, MD, and Paul Barone, MD from the Departments of Pathology at Brooklyn Methodist Hospital and Weill Cornell Medicine, respectively, for their contributions in the preparation and interpretation of all depicted pathology samples included in this case review.

References

- Giani C, Ramone T, Romei C, et al. A New MEN2 Syndrome with Clinical Features of Both MEN2A and MEN2B Associated with a New RET Germline Deletion. *Case Rep Endocrinol*. 2020;2020:4147097. Published 2020 Jul 29. doi:10.1155/2020/4147097
- Gibbons D, Camilleri M, Nelson AD, Eckert D. Characteristics of chronic megacolon among patients diagnosed with multiple endocrine neoplasia type 2B. *United European Gastroenterol J*. 2016;4(3):449-454. doi:10.1177/2050640615611630
- Moore SW, Zaahl M. The Hirschsprung's-multiple endocrine neoplasia connection. *Clinics (Sao Paulo)*. 2012;67 Suppl 1(Suppl 1):63-67. doi:10.6061/clinics/2012(sup01)12
- Wells SA Jr, Pacini F, Robinson BG, Santoro M. Multiple endocrine neoplasia type 2 and familial medullary thyroid carcinoma: an update. *J Clin Endocrinol Metab*. 2013;98(8):3149-3164. doi:10.1210/jc.2013-1204
- Moline J, Eng C. Multiple endocrine neoplasia type 2: an overview. *Genet Med*. 2011;13(9):755-764. doi:10.1097/GIM.0b013e318216cc6d
- Renshaw AA. Sensitivity of fine-needle aspiration for papillary carcinoma of the thyroid correlates with tumor size. *Diagn Cytopathol*. 2011;39(7):471-474. doi:10.1002/dc.21411
- Trimboli P, Treglia G, Guidobaldi L, et al. Detection rate of FNA cytology in medullary thyroid carcinoma: a meta-analysis. *Clin Endocrinol (Oxf)*. 2015;82(2):280-285. doi:10.1111/cen.12563
- Ramachandran MS, Reid JA, Dolan SJ, Farling PA, Russell CF. Laparoscopic adrenalectomy versus open adrenalectomy: results from a retrospective comparative study. *Ulster Med J*. 2006;75(2):126-128.
- Machens A, Dralle H. Biomarker-based risk stratification for previously untreated medullary thyroid cancer. *J Clin Endocrinol Metab*. 2010;95(6):2655-2663. doi:10.1210/jc.2009-2368
- O'Riordain DS, O'Brien T, Grant CS, Weaver A, Gharib H, van Heerden JA. Surgical management of primary hyperparathyroidism in multiple endocrine neoplasia types 1 and 2. *Surgery*. 1993;114(6):1031-1039.
- Raue F, Kraimps JL, Dralle H, et al. Primary hyperparathyroidism in multiple endocrine neoplasia type 2A. *J Intern Med*. 1995;238(4):369-373. doi:10.1111/j.1365-2796.1995.tb01212.x
- Irvin GL 3rd, Deriso GT 3rd. A new, practical intraoperative parathyroid hormone assay. *Am J Surg*. 1994;168(5):466-468. doi:10.1016/s0002-9610(05)80101-1
- American Thyroid Association Guidelines Task Force, Kloos RT, Eng C, et al. Medullary thyroid cancer: management guidelines of the American Thyroid Association [published correction appears in *Thyroid*. 2009 Nov;19(11):1295]. *Thyroid*. 2009;19(6):565-612. doi:10.1089/thy.2008.0403